Applied Nanoscience (2020) 10:4943–4949
https://doi.org/10.1007/s13204-020-01398-8

ORIGINAL ARTICLE

Hybrid solder joints: morphology and shear strength of Sn–3.0Ag–0.5Cu solder joints by adding ceramic nanoparticles through flux doping

A. Aspalter[1] · A. Cerny[1] · M. Göschl[1] · M. Podsednik[1] · G. Khatibi[1] · A. Yakymovych[2] · Yu. Plevachuk[3]

Received: 3 December 2019 / Accepted: 9 April 2020 / Published online: 23 April 2020
© King Abdulaziz City for Science and Technology 2020

Abstract
The shear strength and microstructural evolution of as-cast SAC305 solder joints by addition of various ceramic nanoparticles have been investigated. In contrast to the most popular approach of adding the nano-sized inclusions directly to the SAC solder, the nano-sized Al_2O_3, SiO_2, TiO_2, and ZrO_2 were added to the commercial flux to improve the standard SAC305/Cu joints. In this case, the solder joint was prepared from a sandwich Cu/flux + nanoceramic/SAC305/flux + nanoceramic/Cu. The nanocomposite fluxes with various content (0–1.0 wt%) ceramic nanoparticles (NPs) were employed in our study. The analysis of the microstructure and mechanical properties of the produced hybrid SAC305 solder joints showed several satisfactory modified results. For instance, the growth kinetics of the interfacial Cu–Sn IMC decreased by the addition of Al_2O_3, SiO_2, and ZrO_2 NPs into the flux. The shear stress tests displayed an increase of this mechanical property of the corresponded hybrid solder joints. In contrast, an addition of up to 0.5 wt% nano-TiO_2 increased the growth kinetics of the interfacial Cu–Sn layer. Furthermore, a comparison analysis showed that the most beneficial influence was obtained by minor additions of SiO_2 NPs into the SAC305 solder alloy.

Keywords Solder joint · Ceramic nanoparticles · Microstructure · Shear stress

Introduction

Research and development in the electronics industry have been focusing towards improved or new high-technology products covering a wealth of business areas. In most cases, such specific consumer standards include miniaturization, high performance and good mechanical reliability. For this reason, materials and technologies which are involved in the industrial manufacturing and processes have been continuously developing. In case of the soldering process, one of the most investigated topics is related to an addition of various nano-sized particles into the commercial solder materials to develop a next generation of those. It should be noted that the main focus of these research is put on investigations and characterization of nanocomposite solders and their joints by minor additions of both ceramic and metal nanoparticles into the commercial Sn–Ag–Cu (SAC) solder paste (Tan et al. 2015; Zhang et al. 2019).

For instance, the authors have investigated an impact of various ceramic and metal nano-sized inclusions on microstructure and mechanical properties of the SAC305 solder joint (Yakymovych et al. 2016, 2018a). Furthermore, the changes in the structure as well as in physical and chemical properties of the liquid SAC solder caused by addition of various metal NPs were also investigated (Yakymovych et al. 2018b, c). It should be noted that the solder is reflowed during the soldering process. Therefore, these studies have given essential information to understand and simulate

✉ Yu. Plevachuk
plevachuk@mail.lviv.ua

G. Khatibi
golta.khatibi@tuwien.ac.at

A. Yakymovych
yakymovychandriy@gmail.com

[1] Christian Doppler Laboratory for Lifetime and Reliability of Interfaces in Complex Multi-Material Electronics, Chemical Technologies and Analytics, TU Wien, Getreidemarkt 9/CT-164, 1060 Vienna, Austria

[2] Independent Researcher, Dr. Oswin-Moro-Straße 19, 9500 Villach, Austria

[3] Department of Metal Physics, Ivan Franko National University of Lviv, Kyrylo and Mephodiy Str. 8, Lviv 79005, Ukraine

processes in the SAC nanocomposite solder during soldering; while, the reactive metal NPs are dissolved in the liquid Sn-based SAC matrix.

Other approach to reinforce the commercial SAC solder joints is based on an addition of NPs into the commercial flux. This strategy was firstly exanimated by Haseeb ASMA and his group used a flux doped with various metal NPs, such as Co, Mo, Ni and Ti (Ghosh et al. 2013; Sujan et al. 2014). Based on the obtained results, it was suggested that the morphology and growth of interfacial intermetallic compound layers between the solder and Cu substrate can be successfully controlled even with an addition of up to 0.1 wt% of metal NPs into the flux. We refer such solder/NPs doped flux/substrate joints as "hybrid solder joints".

In the present study, the nanocomposite flux with 0.5 wt% and 1.0 wt% of various ceramic NPs was placed between SAC305 solder foil and Cu substrate providing the maximal concentration of nanoinclusions within the weakest place of the solder joint, namely at the interface solder/substrate. A comparison analysis of the microstructure of the interfacial IMCs layer and the shear stress measurement has been performed.

Materials and methods

Production of hybrid solder joints

The Sn–3.0Ag–0.5Sn (SAC305) solder alloy was synthesized from silver casting grains (99.9% metallic purity), tin ingot (99.998% metallic purity) and copper rod (99.9% metallic purity, all metals from Alfa Aesar, Karlsruhe, Germany). The samples were prepared by heating up to 1173 K accurately weighed amounts of pure components (within ± 0.1 mg) in evacuated and sealed quartz ampoules, and further aging at this temperature during 2 weeks. A SAC305 foil with a thickness of about 50 µm had been formed using a foil rolling mill.

Various NP-doped fluxes were prepared by mechanical mixing method of the commercial Pb-free solder flux (rosin-based Indium no-clean Tacflux 089HF; Indium Co., Milton Keynes, UK) with nominally 0.5 and 1.0 wt% ceramic nanoparticles. For instance, commercially available Al_2O_3, SiO_2, TiO_2, and ZrO_2 nanopowders (average particle size 10–15 nm, TECNAN, Spain; Table 1) were used in the present study. Mechanical dispersion of NPs was achieved by manual stirring of nanoparticles in the flux for approximately 15 min at room temperature.

Table 1 Characteristics of the used ceramic nanopowders (TECNAN 2012)

Material	Particle average size, nm	Specific surface area, 10^3 m^2 kg^{-1}	True density, kg m^{-3}
Nano-Al_2O_3	20–25	65–80	3.99
Nano-SiO_2	10–15	180–270	2.65
Nano-TiO_2	10–15	100–150	4.17
Nano-ZrO_2	10–15	70–110	5.68

The solder joints were produced using 2-mm-thick copper strips as substrates, which were ground and polished with emery paper, soaked in 10% diluted sulfuric acid solution, rinsed in isopropanol. In this case, the sandwich-type Cu/(NP-doped flux)/SAC305/(NP-doped flux)/Cu set-ups were placed in a reflow furnace (LPKF Zelflow RO4) to produce the single shear-lap joints. The joint area was about 3.5 mm·2.0 mm·0.3 mm (Fig. 1).

This method has been described in detail elsewhere (Roshanghias et al. 2016). A reflow temperature profile implemented in the reflow soldering process is presented in Fig. 2. The joint samples were polished afterwards to remove the extruded solder and flux residue from the edges.

A part of the produced joints was thermally aged in an Ecocell furnace at 353 K for 137 h and 496 h.

Fig. 1 Preparation of the hybrid solder joints

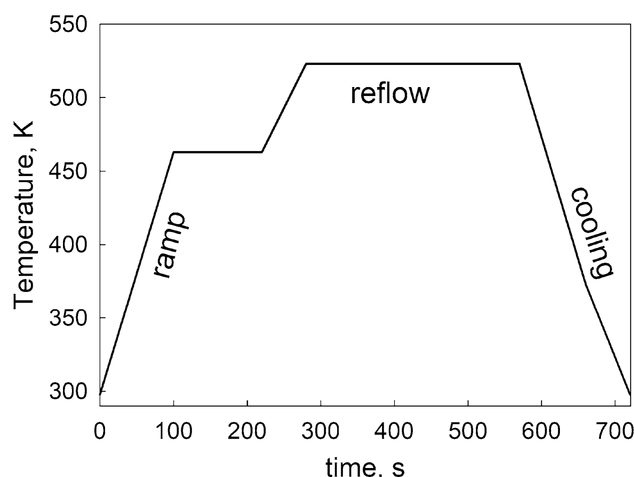

Fig. 2 Reflow temperature profile

Characterization of hybrid solder joints

The shear strength of the solder joint was estimated using a μ-strain tensile machine (ME 30-1, Fuerstenfeld, Austria). The tests were performed at room temperature using a fixed crosshead speed of 2.0 mm min^{-1} and a minimum load resolution of 10 mN. The obtained results were proven to be safe after repeated trials at least three times for each sample condition.

The microstructure of the joints and their fracture surface after the performed shear tests was studied by scanning electron microscopy (SEM-EDX; FEI Quanta 200 and JEOL JSM 6600).

The average thickness of the IMC layer at the interface between the solder and the substrate was calculated using the Digimizer software, freely available in the Internet (MedCalc Software bv 2005–2019).

Results and discussion

Morphology and growth kinetics of interfacial IMCs layer

The cross-sectional micrographs were taken for the as-reflowed hybrid SAC305 solder joins to investigate changes in morphology of the Cu–Sn IMCs layer at the interface solder/Cu caused by minor additions of nano-Al_2O_3, -SiO_2, -TiO_2, and -ZrO_2 to the commercial flux. For instance, the BSE micrographs of the unreinforced SAC305 solder joint and the hybrid SAC305 solder joints with 0.5 wt% Al_2O_3 NPs and SiO_2 NPs are presented in Fig. 3.

As seen in Fig. 3a(I), the interfacial IMC layer of the as-reflowed SAC305 solder joint consisted of Cu_6Sn_5 IMCs; while the typical scallop-type Cu_6Sn_5 grains at the interface solder/Cu extended into the solder matrix. Addition of ceramic nanoparticles led to substantial changes in the morphology of the IMC layer at the interface (Fig. 3b(I) and c(I)). In contrast to our previous studies dealing with nanocomposite Cu/SAC305/Cu solder joints with metal and ceramic nanosized additions (Yakymovych et al. 2016, 2018a), no interfacial Cu_3Sn IMC layer was observed at the investigated solder joints.

The thickness of the interfacial Cu_6Sn_5 IMC layer of the SAC305 solder joint increased after the thermal aging at 453 K for 137 h with a transition from the discontinuous to a more continuous scallop-type form (Fig. 3a(II)). Furthermore, a Cu_3Sn IMC layer is formed between Cu substrate and the interfacial Cu_6Sn_5 IMC layer. The addition of 0.5 wt% of ceramic nanoparticles led to substantial changes in the morphology of the IMC layer towards a more planar type (Fig. 3b(II) and c(II)).

A line-scan analysis of the unreinforced SAC305/Cu solder joint confirmed the presence of a Cu_3Sn layer of about 2.0 μm at the interface zone (Fig. 3IIa); while, the calculated average thickness of the entire interfacial Cu_6Sn_5/Cu_3Sn layer was about 7.1 μm (Table 2).

The changes in average thickness of the interfacial Cu–Sn IMCs layer formed at the Cu/flux/SAC305/flux/Cu by addition of ceramic NPs to the flux are presented in Fig. 4.

As seen from Figs. 3 and 4, minor additions of nano-Al_2O_3 and nano-SiO_2 to the flux changed mainly the morphology of the interfacial IMCs layer of the hybrid SAC305 solder joints; while, the thickness of the IMCs layer slightly decreased to 10% for the 1.0 wt% nano-SiO_2.

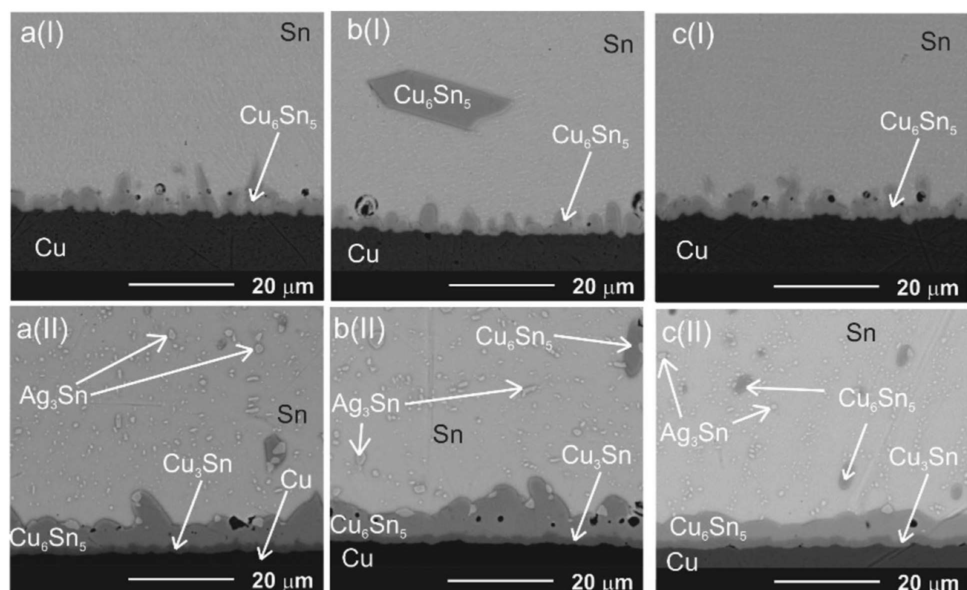

Fig. 3 BSE micrographs of SAC305 (**a**) and SAC305 + 0.5 wt% nano-Al_2O_3 and -SiO_2 (**b** and **c**, respectively) solder joints in as-reflowed condition (I) and after thermal aging at 453 K for 137 h (II)

Table 2 The total average thickness of IMC layers at the interface solder/Cu of the aged solder joints at 453 K for 137 h

NP-doped flux (wt%)		Total average thickness of IMCs layer (μm)	
		Cu_3Sn	$Cu_6Sn_5+Cu_3Sn$
Unreinforced		2.0 ± 0.3	7.1 ± 0.7
Al_2O_3	0.5%	1.8 ± 0.2	7.0 ± 0.5
	1.0%	2.0 ± 0.3	6.5 ± 0.5
SiO_2	0.5%	1.9 ± 0.2	7.0 ± 0.5
	1.0%	2.0 ± 0.3	6.6 ± 0.4
TiO_2	0.5%	1.9 ± 0.3	7.8 ± 0.7
	1.0%	1.7 ± 0.2	6.9 ± 0.6
ZrO_2	0.5%	1.6 ± 0.2	6.6 ± 0.6
	1.0%	1.8 ± 0.3	7.2 ± 0.6

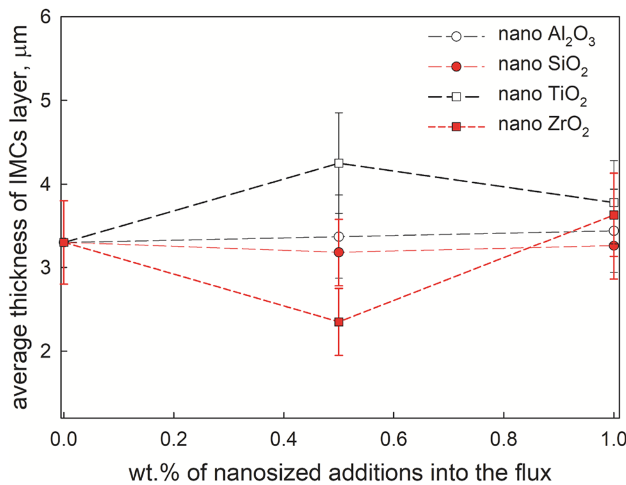

Fig. 4 Average thickness of the interfacial Cu_6Sn_5 IMCs layer formed at the as-reflowed Cu/(NP-doped flux)/SAC305/(NP-doped flux)/Cu

In contrast, additions of 0.5 wt% nano-TiO_2 and nano-ZrO_2 showed an impact on the thickness of the interfacial Cu_6Sn_5 layer, but in the opposite way: a decrease of the thickness in case of the nano-TiO_2, and an increase in case of nano-ZrO_2. Further increase of these ceramic nanoparticles in the flux up to 1 wt% resulted in similar impact, slightly increasing the average thickness of the interfacial Cu_6Sn_5 IMCs layer of the un-reinforced SAC305 solder joint. Based on the presented results, we concluded that an increase of the amount of nano-sized ceramic inclusions in the flux from 0.5 to 1.0 wt% led to less significant changes in the average thickness of the interfacial IMC layer of the as-reflowed hybrid solder joints. Similar tendency, indicated in the nanocomposite SAC305 solder joints, was explained by agglomeration and segregation of NPs during the reflowed process, which led to the decrease in their surface energy and reduced the amount of surface-active NPs (Wang et al. 2015; Yakymovych et al. 2016).

As seen in Fig. 5, the most pronounced decrease in the growth kinetics of the interfacial Cu–Sn layer for as-reflowed and aged solder joints was obtained by addition of up to 1.0 wt% nano-SiO_2 (Fig. 5b), and 0.5 wt% nano-ZrO_2 (Fig. 5d). In contrast, the addition of 0.5 wt% nano-TiO_2 into the flux increased the growth kinetics of the interfacial Cu–Sn layer also of the aged hybrid solder joints, but is less pronounced by increasing the amount of nano-sized inclusions in the flux or/and the aging time (Fig. 5c). The results for the nano-Al_2O_3 were inconsistent and show an increase or decrease in the growth kinetics of the interfacial Cu–Sn layer depending on concentration of nanoinclusions in the flux and aging time (Fig. 5a).

The shear stress investigations

The changes in the microstructure of nanocomposite solder joints described above should also result in changes of the mechanical properties. Therefore, it was decided to investigate the shear stress, as one of the main properties of the joint reliability.

Based on the results presented in Fig. 6, it can be concluded that the shear stress of the as-reflowed SAC305 solder joint increased by initial additions of various ceramic nanoparticles, namely by 0.5 wt% of nano-sized inclusions into the flux. The samples with 1.0 wt% of ceramic NPs showed less pronounced enhance of this mechanical property. This behavior is in agreement with literature related to the investigations of the nanocomposite SAC305 solder joint with CeO_2 NPs postulated a gradual increase in the tensile strength for samples with up to 0.5 wt% ceramic NPs. At the same time, further additions of nano-CeO_2 into the SAC305 solder joint led to deterioration of this mechanical property (Roshanghias et al. 2013). In contrast, the initial addition of nano-TiO_2 lead to a decrease in the shear stress with its further increase for the hybrid solder joint with 1.0 wt% TiO_2 NPs.

The minor nanosized ceramic additions lead to a slight deterioration of this mechanical property after thermal aging of the investigated hybrid solder joints (Fig. 7). It should be noted that an increased amount of ceramic nanoparticles in the SAC305 solder joint can lead to a higher degree of microporosity, which could form fine microscopic cracks, culminating in the failure of nanocomposite SAC solder joints (Tsao 2011).

The EDX analysis of the fractured surface was performed after the shear stress tests to establish the presence of nanosized ceramic inclusions in the solder joints. It was a very challenging topic taking into account minor presence of ceramic NPs in the investigated joints; nevertheless, some metal oxides in the pores of the investigated

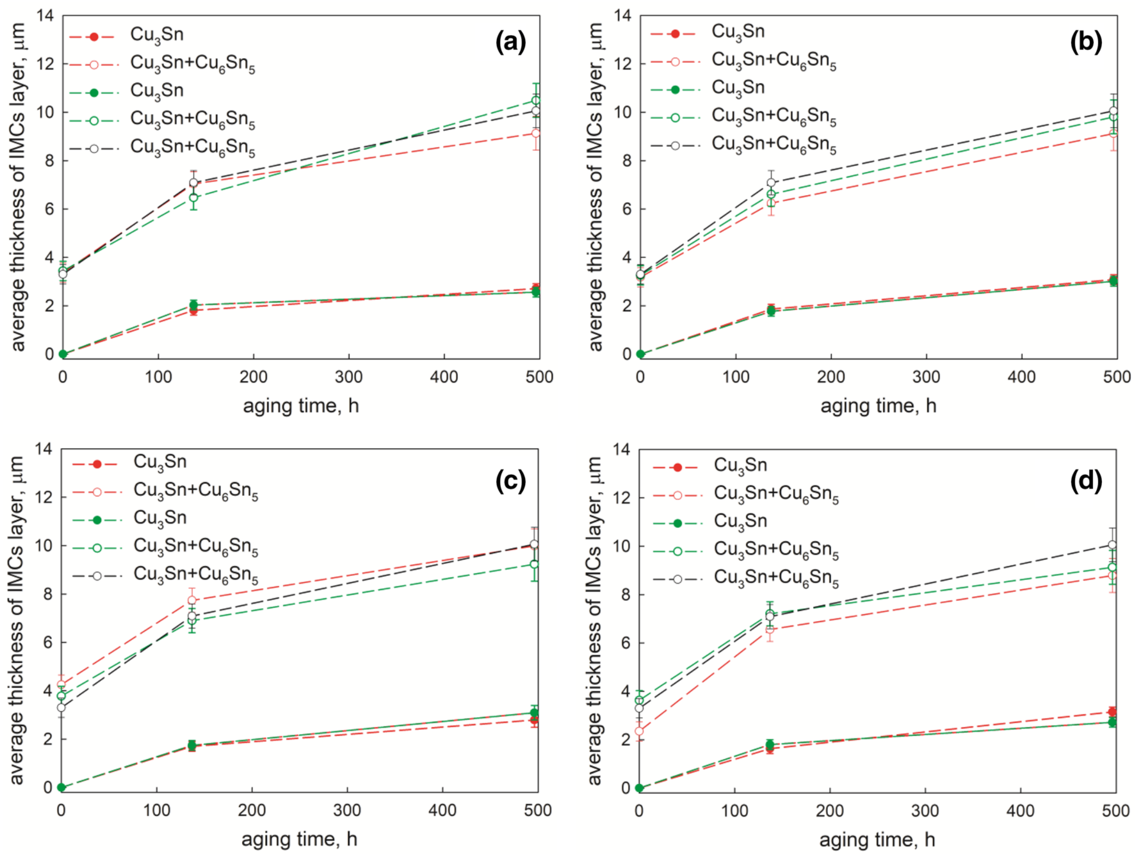

Fig. 5 Average thickness of the interfacial Cu–Sn IMCs layer formed at the aged Cu/(NP-doped flux)/SAC305/(NP-doped flux)/Cu edged at 453 K [(a)—nano-Al_2O_3, (b)—nano-SiO_2, (c)—nano-TiO_2, (d)—nano-ZrO_2; black color—unreinforced flux; red color—0.5 wt%, green color—1.0 wt%]

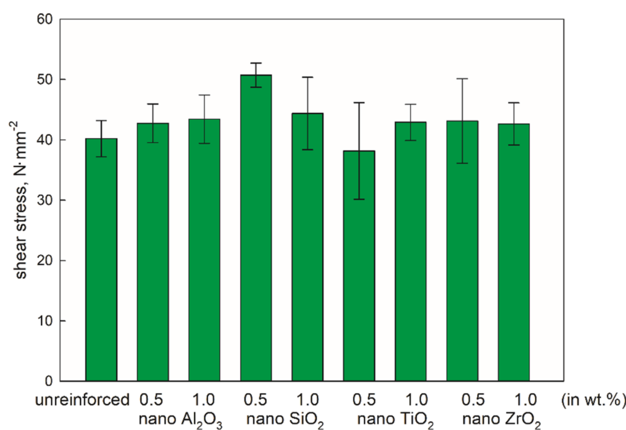

Fig. 6 Shear stress of the as-reflowed hybrid SAC305 solder joins

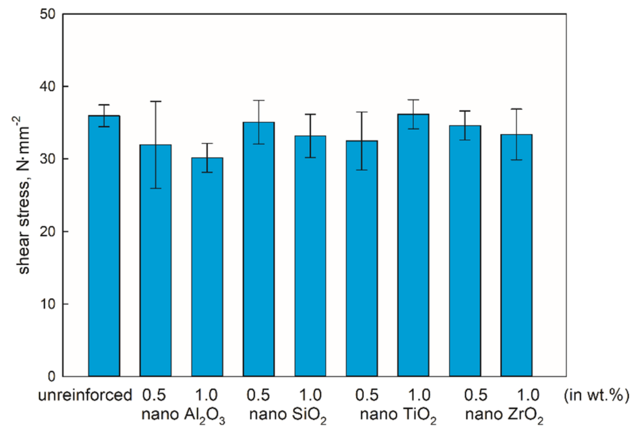

Fig. 7 Shear stress of the hybrid SAC305 solder joins aged at 453 K for 137 h

solder joints were determined. For instance, a presence of Al and Ti was found in the hybrid solder joints reinforced by nano-Al_2O_3 and nano-TiO_2, respectively. As seen in Fig. 8, the results of the EDX analysis for the hybrid solder SAC305 solder joint with 1.0 wt% of nano-TiO_2 showed the presence of Ti in the sample.

Furthermore, a type of fracture can be estimated from the SEM micrographs. Most of our samples showed a ductile type of fracture due to crack propagation within

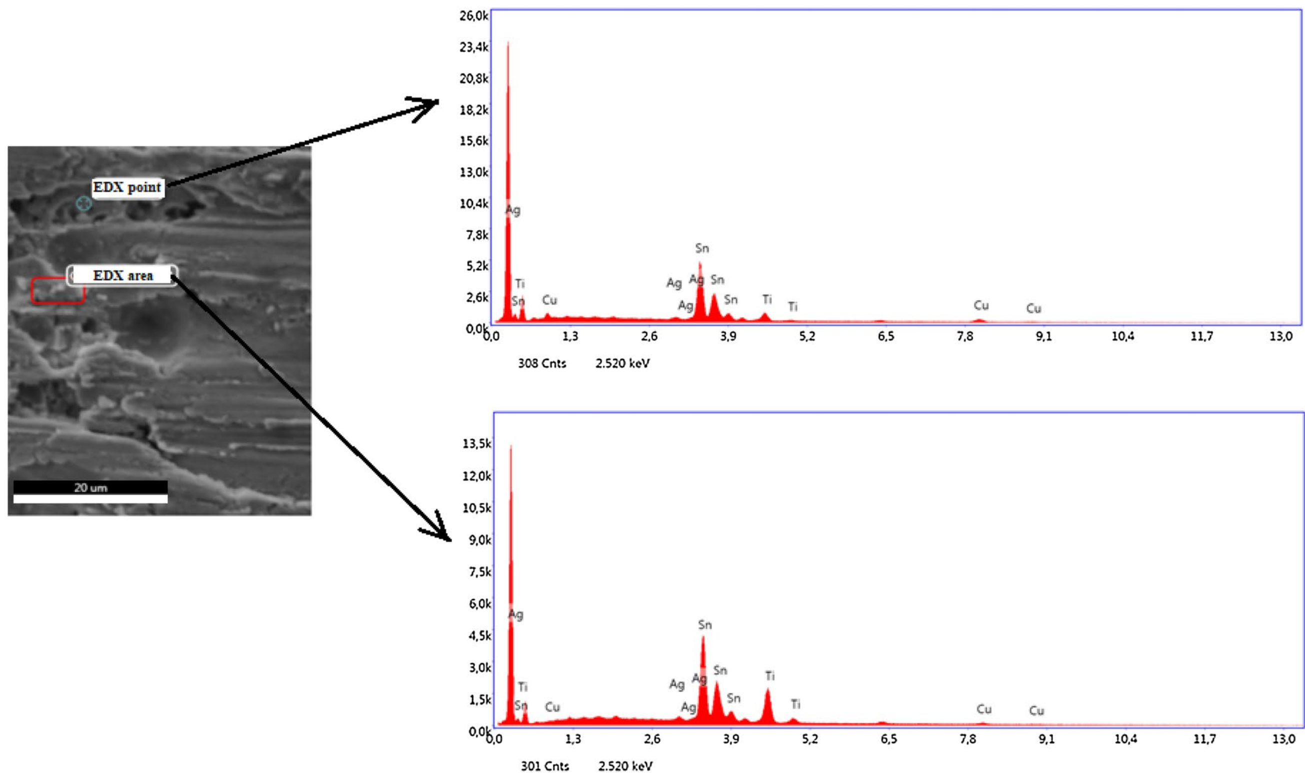

Fig. 8 EDX analysis of the fractured surface of the hybrid SAC305 solder joint with 1.0 wt% nano-TiO_2

the solder joint similar to Fig. 9a. Occasionally, a more brittle fracture was also observed as a result of failure in the vicinity of the interface as presented (Fig. 9b). The differences in the shear stress of the hybrid solder joints such as the indicated decrease in this property by addition of 0.5 wt% nano-TiO_2 into the flux can be explained by formation of the brittle cluster-like regions with a high concentration of ceramic nanoparticles inside the joint (Fig. 9b).

Based on the presented results it can be concluded that initial additions of various ceramic NPs into the flux lead to the changes both in morphology and thickness of the interfacial IMCs layer of the hybrid solder joints. Further increase of the nano-sized ceramic impurities in the flux up to 1 wt% made this effect less pronounced. Similar tendency was indicated also for nanocomoposite SAC305 solder joints using similar ceramic NPs (Yakymovych et al. 2016). Furthermore, a performed comparison analysis of the effects

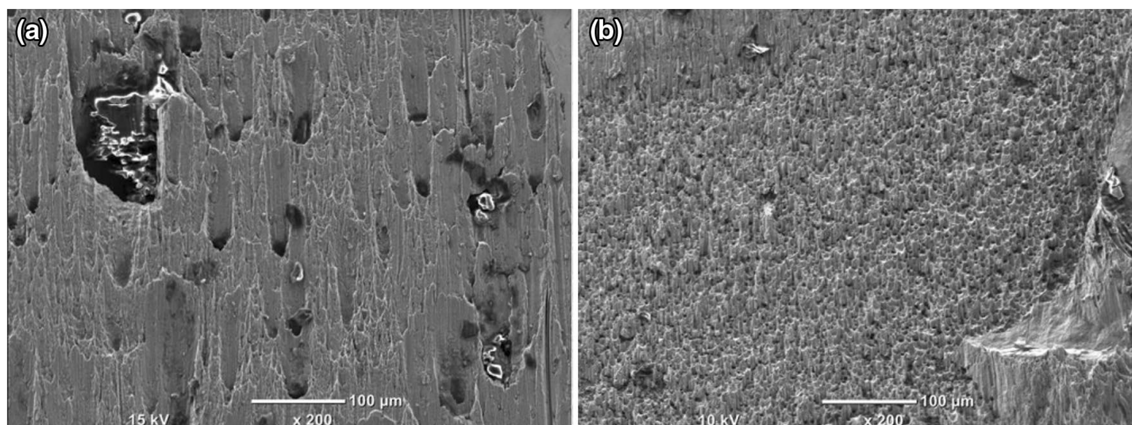

Fig. 9 SEM micrograph of the aged hybrid solder joint with 1.0 wt% nano-SiO_2 (**a**) and as-reflowed hybrid solder joint with 0.5 wt% nano-TiO_2 (**b**)

of minor additions of nano-sized SiO_2, TiO_2, and ZrO_2 NPs into the SAC305 solder paste showed the most improved shear stress of the nanocomposite solder joint with nano-sized SiO_2. Similar to that, the most profound effects on the shear stress of the hybrid SAC305 solder joints were also indicated for the samples with SiO_2 nanoinclusions.

Conclusions

The presented results have shown that initial additions of various ceramic NPs into the flux lead to the changes both in morphology and thickness of the interfacial IMCs layer of the hybrid solder joints. Further increase of the nano-sized ceramic impurities in the flux up to 1 wt% made this effect less pronounced. The comparison analysis of the effects of minor additions of nano-sized SiO_2, TiO_2, and ZrO_2 NPs into the SAC305 solder paste showed the most improved shear stress of the nanocomposite solder joint with nano-sized SiO_2. Similarly, the most profound effects on the shear stress of the hybrid SAC305 solder joints were also indicated for the samples with SiO_2 nanoinclusions.

Acknowledgements The financial support by the Austrian Federal Ministry for Digital and Economic Affairs and the National Foundation for Research, Technology and Development is gratefully acknowledged.

Compliance with ethical standards

Conflict of interest On behalf of all authors, the corresponding author states that there is no conflict of interest.

References

Ghosh SK, Haseeb ASMA, Afifi ABM (2013) Effects of metallic nanoparticle doped flux on interfacial intermetallic compounds between Sn–3.0Ag–0.5Cu and copper substrate. In: IEEE 15th electronics packaging technology conference (EPTC 2013), pp 21–26. https://doi.org/10.1109/EPTC.2013.6745676

MedCalc Software bv (2005–2019) https://www.digimizer.com/index.php

Roshanghias A, Kokabi AH, Miyashita Y, Mutoh Y, Hosseini HR (2013) Formation of intermetallic reaction layer and joining strength in nano-composite solder joint. J Mater Sci 24(3):839–847. https://doi.org/10.1007/s10854-012-0829-z

Roshanghias A, Khatibi G, Yakymovych A, Bernardi J, Ipser H (2016) Sn–Ag–Cu nanosolders: solder joints integrity and strength. J Electron Mater 45(8):4390–4399. https://doi.org/10.1007/s11664-016-4584-4

Sujan GK, Haseeb ASMA, Afifi ABM (2014) Effects of metallic nanoparticle doped flux on the interfacial intermetallic compounds between lead-free solder ball and copper substrate. Mater Charact 97:199–209

Tan AT, Tan AW, Yusof F (2015) Influence of nanoparticle addition on the formation and growth of intermetallic compounds (IMCs) in Cu/Sn–Ag–Cu/Cu solder joint during different thermal conditions. Sci Technol Adv Mat 16:033505. https://doi.org/10.1088/1468-6996/16/3/033505

TECNAN Navarrean Nanoproducts Technology (2012) Catalog, powder nanoparticles, Los Arcos, Navarra, Spain

Tsao LC (2011) An investigation of microstructure and mechanical properties of novel Sn3.5Ag0.5Cu–XTiO_2 composite solders as functions of alloy composition and cooling rate. Mater Sci Eng A 529:41–48. https://doi.org/10.1016/j.msea.2011.08.053

Wang Y, Zhao XC, Xie XC, Gu Y, Liu Y (2015) Effects of nano-SiO_2 particles addition on the microstructure, wettability, joint shear force and the interfacial IMC growth of Sn3.0Ag0.5Cu solder. J Mater Sci 26(12):9387–9395. https://doi.org/10.1007/s10854-015-3151-8

Yakymovych A, Plevachuk Yu, Svec P Sr, Svec P, Janickovic D, Sebo P, Beronska N, Roshanghias A, Ipser H (2016) Morphology and shear strength of lead-free solder joints with Sn3.0Ag0.5Cu solder paste reinforced with ceramic nanoparticles. J Electron Mater 45(12):6143–6149. https://doi.org/10.1007/s11664-016-4832-7

Yakymovych A, Svec P Sr, Orovcik L, Bajana O, Ipser H (2018a) Nanocomposite SAC solders: the effect of adding Ni and Ni–Sn nanoparticles on morphology and mechanical properties of Sn-3.0Ag-0.5Cu solders. J Electron Mater 47(1):117–123. https://doi.org/10.1007/s11664-017-5834-9

Yakymovych A, Weber H, Kaban I, Ipser H (2018b) Dynamic viscosity of a liquid Sn-3.0Ag-0.5Cu alloy with Ni nanoparticles. J Mol Liquid 268:176–180. https://doi.org/10.1016/j.molliq.2018.07.069

Yakymovych A, Kaptay G, Flandorfer H, Bernardi J, Schwarz S, Ipser H (2018c) The nano heat effect of replacing macro-particles by nano-particles in drop calorimetry: the case of core/shell metal/oxide nano-particles. RSC Adv 8:8856–8869. https://doi.org/10.1039/C7RA13643A

Zhang P, Xue S, Wang J, Xue P, Zhong S, Long W (2019) Effect of nanoparticles addition on the microstructure and properties of lead-free solders: a review. Appl Sci 9:2044. https://doi.org/10.3390/app9102044

Publisher's Note Springer Nature remains neutral with regard to jurisdictional claims in published maps and institutional affiliations.